Quantum-mechanical study of vibrational relaxation of HF in collisions with Ar atoms

Roman V. Krems[a] and Nikola Marković
Department of Chemistry, Physical Chemistry, Göteborg University, SE-412 96, Göteborg, Sweden

Alexei A. Buchachenko[b]
Laboratory of Molecular Structure and Quantum Mechanics, Department of Chemistry, Moscow State University, 119899 Moscow, Russia

Sture Nordholm
Department of Chemistry, Physical Chemistry, Göteborg University, SE-412 96, Göteborg, Sweden

(Received 1 September 2000; accepted 27 October 2000)

Vibrational relaxation cross sections and rate constants of HF($v=1$) by Ar are calculated on a recent semiempirical potential energy surface (PES) [J. Chem. Phys. **111**, 2470 (1999)] using the quantum-mechanical coupled states approach. Accurate theoretical estimations of rate coefficients for vibrational relaxation of HF($v=1$) at temperatures between 100 and 350 K are obtained. The vibrational relaxation is shown to be of a quasiresonant character and occur mostly to two nearest rotational levels of the ground vibrational state. The weak isotope effect after substitution of HF by DF is investigated and explained. The cross sections for vibrational relaxation of HF($v,j=0$), where $v=1,2,3,4$, are calculated and shown to increase significantly as v increases. In the same calculations we observe a dramatic increase of multiple quantum vibrational transitions as the difference between the initial and final states falls in close resonance with the collision energy. A comparison of the cross sections obtained from the coupled states calculations with those performed with rotational infinite-order-sudden approximation proves a crucial role of molecular rotations for vibrational relaxation. Finally, we describe the close coupling coupled states calculations for relaxation and rotational excitation of HF($v=1$, $j=0$) with a reduced number of open channels in the basis set and show that it is possible to obtain converged results for rotationally inelastic transitions between the various levels of $v=1$ neglecting all states below $v=1$, $j=0$. © *2001 American Institute of Physics.* [DOI: 10.1063/1.1333704]

I. INTRODUCTION

The interest in the mechanism of vibrational relaxation (VR) of hydrogen halides (HX) is mainly concerned with the participation of vibrationally excited HX molecules in laser systems and chemical reactions with nonstatistical energy partitioning between various degrees of freedom as well as possible formation of inverse rotational population of HX molecules as a result of vibration-to-rotation energy conversion.[1–3] VR of HX molecules in collisions with rare gases (Rg) has also attracted much attention because of experiments on the relaxation in inert matrices. Many gas-phase experiments involving HX molecules use Rg as carrier gases and it is necessary to know the effect of the carrier gas in order to interpret the experimental results.[3,4] A recent interest in VR in atom–diatom collisions, in general, and the Rg+HX collisions, in particular, has been stimulated by observation of quasiresonant vibration–rotation energy transfer.[5,6]

For these reasons, VR of hydrogen halides, and HF in particular, has been a subject of many experimental studies[7–19] whose results are collected and reviewed in a comprehensive work by Leone.[20] VR of HF molecules by Rg is very slow. That is why most experimental studies focus mainly on high temperature regimes. Bott and Cohen[11–13] have measured the temperature dependence of the relaxation times of HF($v=1$) and DF($v=1$) by Ar and He in the interval 1350–4000 K by monitoring infrared emission in shock tubes. An interesting result of their study was that the relaxation times for DF were almost the same as those for HF and the difference between the results for HF and DF was within the experimental uncertainty. Blair *et al.*[14] used the shock tube—laser induced fluorescence method, to study VR of HF by Ar at temperatures 800–2400 K. In general, their data were in an agreement with those by Bott and Cohen although they found that the relaxation times of HF by Ar were so small that low amounts of impurities influence them significantly even at as high a temperature as 1000 K. The measurements of VR in HX by Rg at lower temperatures[7–10] can, therefore, be considered only as upper limits of the true values. Smith and Wrigley[15,16] used a time resolved vibrational chemiluminescence method to measure the relaxation of HF($v=2,3,5$) by various agents including Ar. They found that the relaxation rate increases significantly with v and the rate constant can be scaled to a good approximation as v^n where n ranges between 2.0 and 3.8 depending on the deactivating agent. Several experimental studies of

[a]Telefax: +46-31167194. Electronic mail: roman@phc.chalmers.se
[b]Currently on sabbatical leave at IMAFF CSIC, Madrid, Spain.

vibrationally elastic rotational relaxation in HF by Rg[3,21,22] have been performed in order to elucidate the detailed collisional energy transfer processes. BelBruno *et al.*[21] used the measurements of the argon-broadened HF linewidths to obtain state-to-state rotation relaxation rate constants. Taatjes and Leone[3] reported a study of HF($v=0, j=13$) relaxation by various Rg atoms. Recently, Chapman *et al.*[22] conducted measurements of state-to-state rotationally inelastic cross sections at three collision energies. To summarize, the experimental findings were that (1) VR of HX (HF) by Rg (Ar) is very slow, (2) there is no or only a small isotope effect when HF is replaced by DF, (3) the VR rate increases rapidly with initial vibrational excitation, (4) low-temperature experimental data on VR are unreliable although there are some accurate measurements of vibrationally elastic rotational relaxation.

These interesting features attracted the attention of theoreticians. However, most theoretical studies of VR in HX molecules are of model character and involve many approximations.[23–35] Moore[23] suggested a model assuming that most of the vibrational energy of the diatomic was converted to rotational energy after a collision with Rg. This provided an explanation of the small isotope effect observed in experiments. A more accurate breathing spheres—effective mass model was subsequently proposed by Nikitin.[24] According to this model the vibrational transition is determined by the relative velocity component directed along the gradient of the PES for interaction of Rg with HX. Within a free rotating model[25–28] it was assumed that rotational transitions in a free rotating diatom are induced by a time-dependent interaction with the collider. The advantage of the model studies was that they provided analytical expressions for VR rate constants. Thompson[29,30] performed quasiclassical trajectory (QCT) calculations of VR in HF and HCl by Ar. For the case of HF his results showed that the rotational energy transfer is almost independent of the vibrational excitation, whereas the vibrational transitions are significantly enhanced by increasing rotational energy. He also argued that both the rotational and vibrational energy of HF for the v and j quantum numbers considered are predominantly converted into translational energy of the fragments. This suggestion is in apparent contradiction to the results of preceding experimental and theoretical studies as well as his QCT calculations of VR in Ar+HCl collisions. Sewell *et al.* performed a combined classical trajectory—quantum scattering analysis of VR of HCl by Ar.[35] It was shown in their work that the effective mass approach to VR can give a reasonable description of vibrational transitions in HCl. The main deductions that can be made from the model and QCT studies of VR are the following: (1) the temperature dependences of the VR rate constants obey the Landau–Teller law ($\sim\exp[-a/T^3]$) to a very good approximation, (2) the VR rates are very sensitive to the intermolecular Rg–HX potential, (3) the rotations of the diatom play a crucial role in the VR process, (4) rotational excitation enhances VR, (5) cross sections for VR are reasonably well described by an exponential energy gap law. These features make the accurate study of VR in HX molecules computationally difficult and the only fully quantum mechanical studies of VR in the HX +Rg systems have been those by Gianturco *et al.*[31–33] and Bienieck.[34] These works are based on either breathing sphere or infinite-order-sudden approximations of the molecular rotation.

Another obstacle for theoretical studies of VR in the Rg +HX systems beyond the computational difficulty has been the lack of reliable three-dimensional interaction potential energy surface (PES). In the previous works the PES' for interaction of Rg with HX were either approximated by a pairwise additive function[29] or by an analytical fit of the *ab initio* data in a limited region of the coordinate space.[24,28,32] However, implementation of an accurate PES seems to be a necessary condition for a quantitative description and qualitative understanding of the VR process. As follows from the numerous microwave and infrared spectroscopic studies of the RgHX van der Waals complexes (see, e.g., Refs. 36 for ArHF), their PES' themselves exhibit quite interesting behavior. First, they are extremely anisotropic having two minima in the collinear configurations. Second, the interaction strength increases with the elongation of HX bond, or, equivalently, with increasing vibrational excitation of the diatomic fragment. Spectroscopic and other experimental data were used by Hutson for construction of accurate semiempirical PES' including the H6(4,3,2) potential for ArHF.[37] Unfortunately, these PES' do not depend on HX bondlength r explicitly, being parameterized by vibrational quantum number v, and can not be used, without additional approximations, in the accurate dynamical calculations of the VR dynamics. Nor have the numerous *ab initio* calculations, which showed impressive agreement with the semiempirical approach,[38] so far provided a global PES suitable for these purpose. However, Grigorenko *et al.*[39] suggested a simple diatomics-in-molecule (DIM) model for the ArHF PES. Being refined to fit the spectroscopic data,[40] this potential has been shown to provide very reasonable description of the vibrational predissociation of the ArHF complex[40,41]—a rupture of a van der Waals bond due to the vibrational energy transfer from the excited diatomic fragment, a process which can be considered as a ''half-collision'' analog of the VR process. Vibrational predissociation dynamics is more sensitive to the topology of the PES than the collision dynamics which is primarily related to the repulsive part of the interaction and subjected to averaging over the mutual orientations of the fragments and the total angular momentum to a greater extent. Previous experience[42] leads us to expect that the DIM potential from Ref. 40 will provide a reliable description of the Ar+HF vibrational relaxation. Another advantage of implementing this PES is the possibility of direct comparison of the qualitative features of full- and half-collision vibrational energy transfer.

The main goal of the present paper is to improve our understanding of the VR mechanism in the Ar+HF collisions. For this purpose we use the most suitable quantum-mechanical method—a close coupling coupled states (CC-CS) approach[43–48]—for the dynamical calculations on the DIM PES.[40] Treating both rotational and vibrational degrees of freedom of the diatom accurately we examine the qualitative peculiarities of the VR observed in the high-temperature experiments[11–19] and use the low-temperature experimental

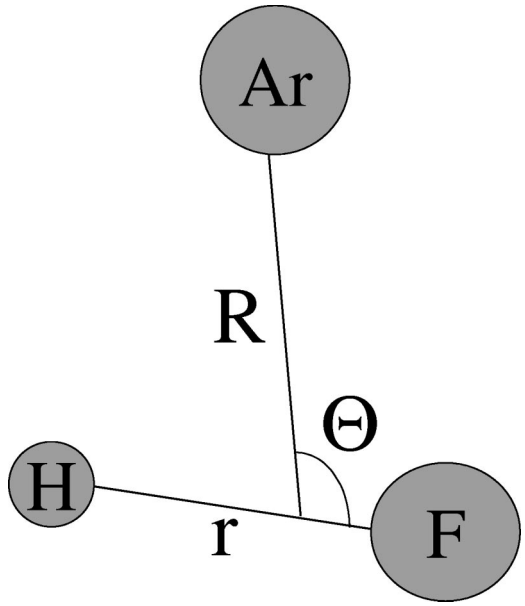

FIG. 1. Jacobi coordinates for internal structure of the Ar+HF complex.

data on vibrational[7,9] and rotational[3] relaxation of HF by Ar to test our approach. In order to investigate the role of molecular rotations in VR we perform cross section calculations with an infinite-order-sudden approximation for rotations of the diatom. Extending our CC-CS calculations to as high energies as possible we investigate the one and multiple quantum VR from the excited vibrational levels of HF. Finally, we perform some additional quantum-mechanical calculations on an approximate pairwise PES in order to study the dependence of the results upon the interaction potential.

The following notation is used for quantum numbers in the present paper: J denotes the total angular momentum for the collision, while j is the rotational angular momentum of the diatom. $\hat{J}_z$ and $\hat{j}_z$ are the operators that give the z component of $\hat{J}$ and $\hat{j}$, respectively, and Ω denotes the projection of the total angular momentum on the body-fixed quantization axis. The notation v is used to denote the vibrational states of the diatom. The hat over a symbol denotes the corresponding operator. Conventional Jacobi coordinates are used to describe the internal dynamics of the triatomic system as shown in Fig. 1. The remainder of the paper is organized as follows. In Sec. II we describe the dynamical methods that we use for the scattering calculations. Section III presents the results and their discussion while the conclusions are summarized in Sec. IV.

II. SCATTERING CALCULATIONS

In our work we implement (in atomic units) the approach developed by McGuire and Kouri[43] and used by many authors to describe the dynamics of the ro-vibrational energy transfer in atom–diatom collisions.[44–46,48] In brief, the coupled states approximation (CSA) is applied in a body-fixed coordinate system with the quantization axis coinciding with the line between the centers of mass of the colliding particles R. The centrifugal term in the total Hamiltonian of the triatomic system is approximated as[43,46]

$$(\hat{J}-\hat{j})^2=\hat{J}^2+\hat{j}^2-2\hat{J}_z\hat{j}_z. \tag{1}$$

In this expression the terms responsible for the coupling between states with different Ω values are omitted. The partial wave functions ($\Psi^{J\Omega}$) are expanded in terms of products of translational ($F_{vj}^{J\Omega}$), vibrational (χ_v^j) and rotational ($Y_{j\Omega}$) functions as follows:

$$\Psi^{J\Omega}=\frac{1}{R}\sum_{v,j} F_{vj}^{J\Omega}(R)\chi_v^j(r)Y_{j\Omega}(\Theta,0). \tag{2}$$

Substitution of expansion (2) into the stationary Schrödinger equation results in a system of close coupling coupled states (CC-CS) equations to be solved for fixed values of J and Ω

$$\left[\frac{d^2}{dR^2}+k_{vj}^2-\frac{J(J+1)+j(j+1)-2\Omega^2}{R^2}\right]F_{vj}^{J\Omega}(R)$$

$$=2\mu\sum_{v',j'}\langle vj\Omega|V(r,R,\Theta)|v'j'\Omega\rangle F_{v'j'}^{J\Omega}(R). \tag{3}$$

Here μ is the reduced mass of the colliding particles, $k_{vj}=\sqrt{2\mu(E-\epsilon_{vj})}$, E is the total energy and ϵ_{vj} is the energy of the ro-vibrational channel $|vj\rangle$. We will omit Ω notation from the designation of the diatomic states where it is not necessary. In order to evaluate the matrix elements $\langle vj\Omega|V(r,R,\Theta)|v'j'\Omega\rangle$ the interaction potential is conventionally expanded in Legendre polynomials as

$$V(r,R,\Theta)=\sum_{\lambda} V_\lambda(r,R)P_\lambda(\cos(\Theta)), \tag{4}$$

and the integrals over the angular part are taken analytically.[49] The asymptotic solution of Eq. (3) yields the scattering S-matrix that is used for calculation of the total cross sections for inelastic ro-vibrational transitions according to the expression

$$\sigma_{vj\to v'j'}^{\Omega}(E)=\frac{\pi}{k_{vj}^2}\sum_J (2J+1)|S_{vj;v'j'}^{J\Omega}(E)|^2. \tag{5}$$

Averaging of $\sigma_{vj\to v'j'}^{\Omega}(E)$ over a Maxwell–Boltzmann distribution of energies and summation over all helicities Ω gives state-resolved rate constants ($k_{vj\to v'j'}$) which are summed over all final rotational states and averaged over all initial rotational states with Boltzmann weighting factors. The obtained quantity ($k_{v\to v'}$) corresponds to the experimentally observed rate constant.

Apart from the CSA [Eq. (1)] we make no other approximations, i.e., the vibrational wave functions χ_v^j and the corresponding ro-vibrational energy levels of the diatomic molecule are determined numerically by solving the equation

$$\left[-\frac{1}{2\mu_{\rm HF}}\frac{d^2}{dr^2}+V_{\rm HF}(r)+\frac{j(j+1)}{2\mu_{\rm HF}r^2}\right]\chi_v^j(r)=\epsilon_{vj}\chi_v^j(r), \tag{6}$$

where $\mu_{\rm HF}$ denotes the reduced mass of the diatomic and the spectroscopic potential $V_{\rm HF}(r)$ has been taken from Ref. 50 in the form of an extended Rydberg function.

In order to investigate the role of molecular rotations in VR we, following the works of Banks and Clary[46] and Tanner and Maricq,[48] perform the calculations using the close

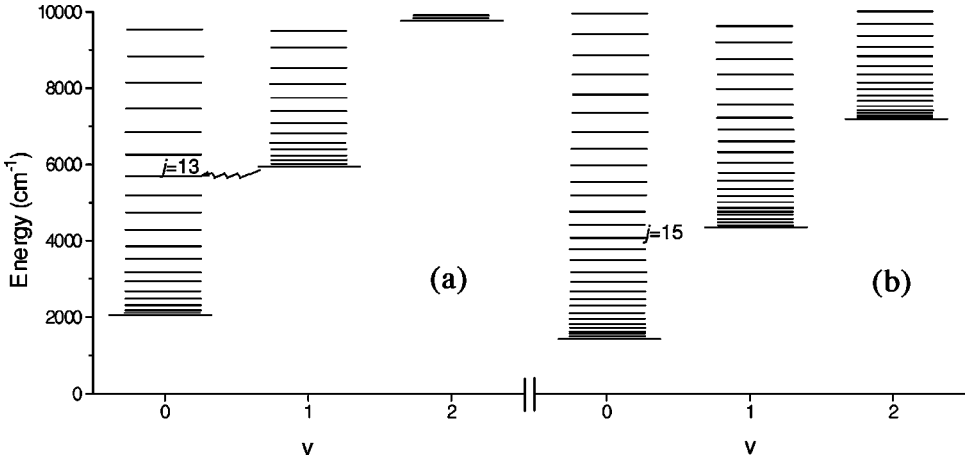

FIG. 2. Ro-vibrational energy level diagram of HF (a) and DF (b).

coupling method for the vibrational degree of freedom and the infinite-order-sudden approximation for rotations of the diatom (CC-IOSA). In the CC-IOSA the energy sudden approximation is made to the centrifugal term in the total Hamiltonian

$$(\hat{J}-\hat{j})^2=\hat{J}^2+\hat{\bar{J}}^2. \tag{7}$$

Here $\bar{J}$ denotes an effective j value often chosen to be equal to zero.[45,46,48] The total Hamiltonian of the triatomic system depends on the Jacobi angle Θ only parametrically through the intermolecular interaction potential and the partial wave expansion now becomes

$$\Psi^{J\Omega}=\frac{1}{R}\sum_v F^J_{vJ}(R,\Theta)\chi^{\bar{J}}_v(r). \tag{8}$$

This leads to the following CC-IOSA equations to be solved with fixed values of J and Θ:

$$\left[\frac{d^2}{dR^2}+k^2_{v\bar{J}}-\frac{J(J+1)+\bar{J}(\bar{J}+1)}{R^2}\right]F^J_{vJ}(R,\Theta)$$

$$=2\mu\sum_{v'}\langle v|V(r,R,\Theta)|v'\rangle F^J_{v'\bar{J}}(R,\Theta). \tag{9}$$

The solution of these equations gives an angle dependent S-matrix ($S^{J,\bar{J}}_{vv'}(\Theta)$) from which the CC-IOSA cross sections can be computed as

$$\sigma_{v\to v'}=\frac{\pi}{2k^2_{v\bar{J}}}\sum_J(2J+1)\int_0^\pi d\Theta\sin\Theta|S^{J,\bar{J}}_{vv'}(\Theta)|^2. \tag{10}$$

Three-dimensional DIM PES for the interaction of HF with Ar is described in Refs. 39 and 40. In order to test the sensitivity of the dynamical results to the interaction potential we perform selected calculations on an approximate PES that is a sum of two pairwise ArH and ArF terms each fitted to *ab inito* second-order Møller–Plesset (MP2) calculations by a modified Buckingham function.[51] This PES will be denoted hereafter as pairwise additive Bunkingham (PAB) PES.

All dynamical calculations presented below are performed using a newly developed program for exact and approximate quantum-mechanical calculations of cross sections for ro-vibrational energy transfer in atom–diatomic molecule collisions. The performance of the code has been checked against a large number of inelastic scattering data available in the literature as well as against selected calculations with the MOLSCAT[52] program. Several methods of propagation of the close coupling equations are employed in the program. More details about our program can be found on the web[53] or requested from the corresponding author.

III. RESULTS

An examination of Fig. 2(a) depicting the ro-vibrational energy diagram of the HF molecule shows that there are 14 rotational levels $|v=0,j\rangle$ below the first vibrational energy threshold and the state $|v=0,j=13\rangle$ is in approximate resonance with the state $|v=1,j=0\rangle$. This diagram as well as the previous theoretical studies suggest that there should be a strong interplay between rotational and vibrational motion of the diatom in the course of an Ar+HF collision.

To obtain cross sections for $|vj\rangle\to|v'j'\rangle$ transitions the CC-CS calculations are performed for $j+1$ helicities $\Omega=0,1,\ldots,j$. A 1% cross-section convergence with respect to the number of partial waves and the basis set size is checked and ensured. We find that at least two closed vibrational states should be included in the basis set to have the vibrationally inelastic cross sections fully converged. To obtain the total rate constant for relaxation of the $v=1$ state at $T=350$ K cross section calculations are performed for 10 initial j values in the energy interval 5–4000 cm^{-1}.

Although many early studies of the validity of the CS approximation for the atom–diatomic molecule scattering calculations (see, e.g., Refs. 43 and 54) involved systems with low anisotropy of interaction, recent calculations for the collisions of He with CO and the collisions of Ar and He with OH[55–57]—systems possessing high anisotropy of interaction—showed a good agreement of the CS results with both more accurate coupled channel calculations and experimental data where available. In the case of Ar+HF collisions the CS approximation was investigated by Barrett and co-workers[58] who performed a semiclassical study of rotationally inelastic scattering on the H6 PES[37] which is similar to the PES we use in the present work. The authors[58] found that the CSA results agreed very well with their full

TABLE I. Equilibrium distances and interaction energies on the DIM and PAB PES' of the ArHF complex at the HF interatomic distance 0.9186 Å and fixed values of Θ. The entries given in italic correspond to the true minima of the PES'. The energy is referred to the separation limit of Ar and HF. The value $\Theta=0$ corresponds to the collinear Ar+HF approach.

PES	Θ (deg)	R (Å)	E (cm^{-1})
DIM	*0*	*3.585*	*−159.0*
	90	3.471	−88.5
	180	*3.304*	*−118.6*
PAB	*0*	*3.492*	*−173.2*
	90	3.329	−106.0
	180	3.465	−74.3

semiclassical calculations. To evaluate the error of the CSA in the present work we also perform full close coupling calculations of cross sections for multiple quantum rotational transitions in the HF($v=0, j=0$)+Ar collisions. Our results show that in the range of collision energies between 200 and 3000 cm^{-1} the average deviation of the CS values from the CC calculations is within 20% of the absolute magnitude of the cross section.

To study the dependence of the dynamical results upon the intermolecular interaction potential we complement selected calculations of the vibrationally elastic and inelastic cross sections on the DIM PES with those performed on the PAB PES. The radial (R) dependence of the two PES' at large intermolecular separation is qualitatively the same in the collinear and T-shaped configurations (Table I). The angular (Θ) dependence is, however, different. In agreement with experimental and *ab initio* data on the ArHF van der Waals complex,[36–38] DIM PES has two minima in the collinear configurations $\Theta=0$ and 180°, whereas there is only one minimum on the PAB PES at $\Theta=0$. At short intermolecular distances the PAB PES overestimates the DIM interaction strength by a factor 3.5–3.7 in the collinear Ar–HF configuration ($\Theta=0°$) and underestimates the interaction steepness by 1.5 times in the collinear Ar–FH configuration ($\Theta=180°$). In the T-shaped configuration ($\Theta=90°$) both PES are similar differing by a factor 1.1–1.2. The DIM PES shows stronger dependence on the HF interatomic distance r than the PAB PES. At large r values (>4.5 Å) the interaction energy on the DIM PES is 1.5–2 times greater than that on the PAB PES and the difference becomes greater as r increases. The different short range behavior and Θ-dependence of the DIM and PAB PES' lead to significantly different Legendre expansions (4) of the PES'. The DIM PES is more anisotropic than the PAB one. At least 25 terms in Legendre expansion (4) of the DIM PES are necessary to obtain the fully converged cross sections for vibrationally inelastic transitions whereas it is sufficient to retain 20 terms in the expansion (4) of the PAB PES. The first terms of the PAB PES expansion differ from the corresponding terms of the DIM PES expansion by more than an order of magnitude. The DIM PES is used for most calculations, while the PAB PES is implemented mainly for the purpose of comparative analysis of the most interesting features of the dynamics. In the discussion below, theoretical results correspond to the calculations with the DIM PES unless stated otherwise.

TABLE II. Rate constant ($cm^3\ s^{-1}$ molecule^{-1}) for rotational relaxation of HF($v=0, j=13$) by Ar at room temperature.

	$k_{v=0,j=13\rightarrow v=0,\Sigma j'}$
DIM PES	1.71×10^{-12}
PAB PES	0.59×10^{-12}
Experiment (Ref. 3)	$0.93(\pm0.09)\times10^{-12}$

We start by performing calculations of the rate constant for rotational relaxation of HF($v=0, j=13$) by Ar (Table II) that has been measured accurately by Taatjes and Leone.[3] The difference between the measured and calculated values is within the variations of the PES' which reflects their distinct anisotropy. It may be interesting to note that similar calculations of the relaxation rate constant in HF($v=0, j=13$)+Ne underestimate the experimental result by a factor of 3.[47]

Table III collects room temperature rate constants for VR of various $|v=1, j\rangle$ states summed over j'. The relaxation rate increases rapidly with initial rotational excitation. The rate constant for VR from $|v=1, j=8\rangle$ is almost two orders of magnitude larger than that for VR of $|v=1, j=0\rangle$. The total rate constant for relaxation of $|v=1\rangle$ in the temperature interval 100–350 K is presented in Table IV. The results agree well with experimental data given that the latter can be considered only as upper bounds of the true values. The rate constant decreases by almost two orders of magnitude as the temperature falls from 350 to 100 K. This is partially due to the rapid decrease of the relaxation rate as the initial rotational distribution gets colder.

TABLE III. Room temperature rate constants ($cm^3\ s^{-1}$ molecule^{-1}) for vibrational relaxation of HF($v=1, j$) by Ar.

j	$k_{v=1,j\rightarrow v=0}$
0	0.088×10^{-15}
1	0.164×10^{-15}
2	0.168×10^{-15}
3	0.260×10^{-15}
4	0.711×10^{-15}
5	1.528×10^{-15}
6	2.079×10^{-15}
7	4.990×10^{-15}
8	5.728×10^{-15}

TABLE IV. Rate constant for vibrational relaxation of HF($v=1$) by Ar, $cm^3\ s^{-1}$ molecule^{-1}. The experimental values are taken from the references indicated in the third column.

T (K)	$k_{v=1\rightarrow v=0}$	Reference
100	7.16×10^{-17}	This work
200	4.08×10^{-16}	This work
300	1.55×10^{-15}	This work
	$<1.90\times10^{-15}$	Refs. 8 and 9
350	2.60×10^{-15}	This work
	$<3.10\times10^{-15}$	Ref. 10
	$<1.10\times10^{-14}$	Ref. 7

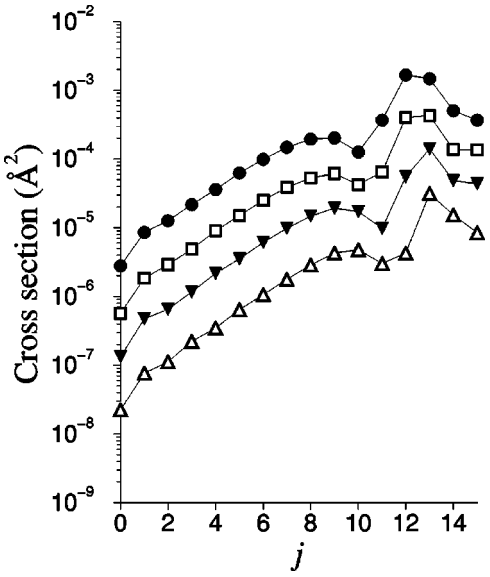

FIG. 3. Cross sections for one quantum relaxation of HF$(v,j=0)$ by Ar: $v=1$ (up triangles), $v=2$ (down triangles), $v=3$ (squares), $v=4$ (circles).

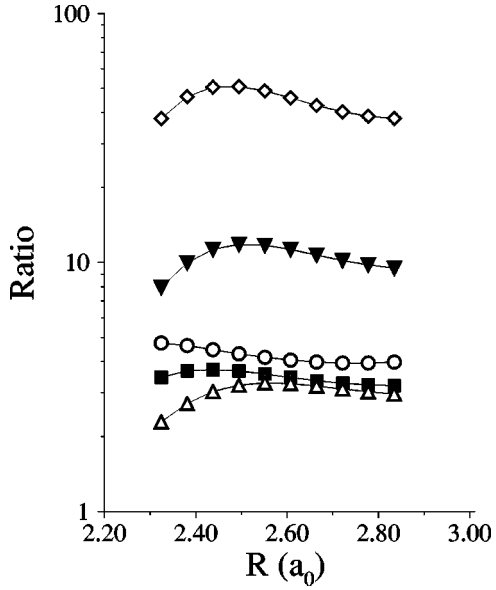

FIG. 4. Ratios of the interaction potential coupling matrix elements as a function of intermolecular separation: Up triangles—$V_{4,3}/V_{3,2}$, squares—$V_{3,2}/V_{2,1}$, circles—$V_{2,1}/V_{1,0}$, down triangles—$V_{4,3}/V_{2,1}$, diamonds—$V_{4,3}/V_{1,0}$, $V_{v',v''}=\langle v',j=0|V|v'',j=13\rangle$, $\Omega=0$.

Figure 3 depicts logarithmic plots of state-resolved cross sections for one-quantum relaxation of the vibrational levels with initial $v=1,2,3$, and 4 vs the final j values. Interestingly, all curves have similar shape showing resonant peaks around $j=12,13$ for the relaxation from higher v states. The cross sections for VR of $|v=4\rangle$ are almost two orders of magnitude larger than those for VR of $|v=1\rangle$. That can not be explained simply by the anharmonicity of the potential well of HF. The difference between the $|j=0\rangle$ states of $|v=4\rangle$ and $|v=3\rangle$ is only a factor 1.7 less than that between $|v=1\rangle$ and $|v=0\rangle$. The distance between the curves for the relaxation of different v states to $|v-1\rangle$ is approximately the same decreasing slightly as v goes up and the total VR cross sections scale approximately as $v^{3.44}$. This is in accord with the experimental observation[4,13,15] that the rate constant for one-quantum VR scales as v^n where v is the number of the initial vibrational state and n is a constant ranging from 2.0 to 3.8 depending on the bath gas. Figure 4 shows plots of the ratios of the coupling matrix elements $\langle j=0,v|V|v-1,j=13\rangle/\langle j=0,v-1|V|v-2,j=13\rangle$ in the region of R values where the coupling matrix elements have the maximum absolute magnitude. The ratios $\langle j=0,v|V|v-1,j=13\rangle/\langle j=0,v-1|V|v-2,j=13\rangle$ are approximately 3–5 which is the result of the rapid increase of the interaction energy with the elongation of the HF bondlength. To verify this we perform the calculations of the VR cross sections from the high v levels of HF on the PAB PES that exhibits a weaker dependence on the r-coordinate. The ratios of the coupling matrix elements $\langle j=0,v|V_{PAB}|v-1,j=13\rangle/\langle j=0,v-1|V_{PAB}|v-2,j=13\rangle$ are around 1.5–2.8 (cf. 3–5 with the DIM PES) and the cross sections calculated on the PAB PES increase slower with initial vibrational excitation than those obtained on the DIM PES. The total VR rate of $|v=4,j=0\rangle$ is only 25 times greater than that of $|v=1,j=0\rangle$ (cf. 68 with the DIM PES).

As follows from Fig. 2(a) and the energy gap law[29] the vibrational relaxation of $|v=1\rangle$ in HF should result in an enhanced population of rotationally excited ($j\geqslant 13$) states of $|v=0\rangle$. On the other hand, as it is shown on Fig. 5, the potential coupling due to the interaction of HF with Ar decreases as the difference between the final and initial rotation quantum numbers becomes smaller with the integral $\langle v=0,j=13|V|v=1,j=0\rangle$ having much lower magnitude than that of $\langle v=0,j=0|V|v=1,j=0\rangle$. Figure 6 presents plots of the cross sections for the $|v=1,j=0\rangle\rightarrow|v=0,j\rangle$ transitions vs the final j values at four collision energies. It may be seen that at low collision energies the vibrational transitions are of purely resonant character with $j=13$ and $j=14$ being the only levels populated after the collision. At

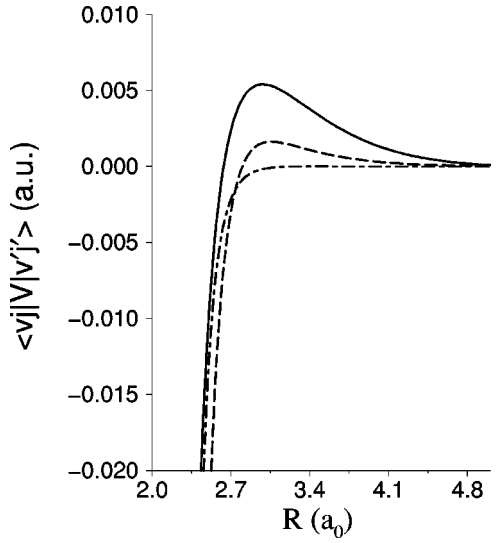

FIG. 5. Interaction potential coupling matrix elements of HF+Ar as functions of the center-of-mass separation: solid line—$\langle v=1,j=0|V|v=0,j=0\rangle$, dashed line—$\langle v=1,j=0|V|v=0,j=7\rangle$, dotted–dashed line—$\langle v=1,j=0|V|v=0,j=13\rangle$.

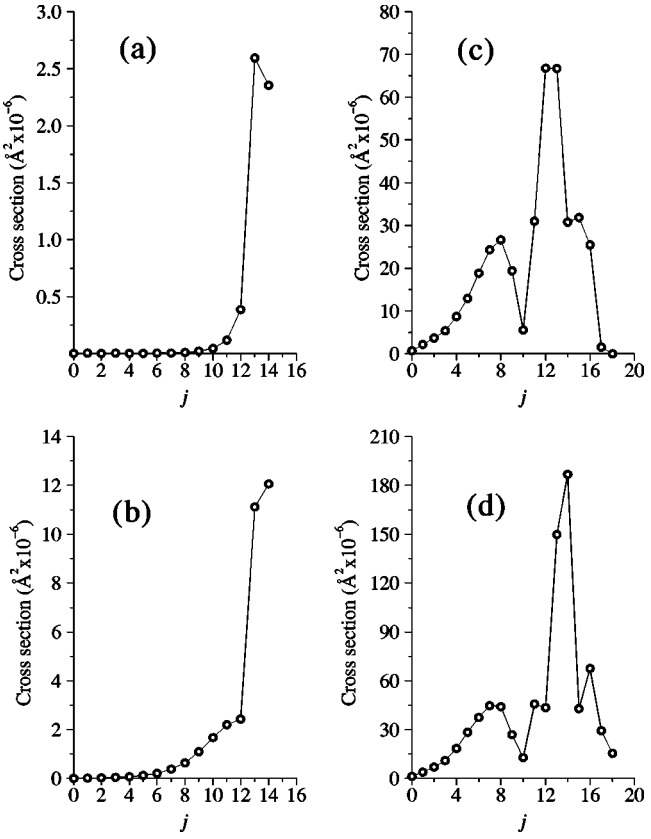

FIG. 6. Cross sections for $|v=1, j=0\rangle \rightarrow |v=0, j\rangle$ transitions in Ar+HF at the collision energies 300 cm^{-1} (a), 834 cm^{-1} (b), 3000 cm^{-1} (c), and 4000 cm^{-1} (d).

higher energies the plots show some structure with additional peaks at $j=6-8$ and $j=16$. These may be explained by the competition of the energy gap law with the coupling due to the interaction of HF with Ar. At low energies the energetic factor prevails and none of the states except $j=13$ and $j=14$ are accessible. But even at higher energies where the resonance peaks are not so pronounced the population of the $j=13$ and $j=14$ levels dominates. This peculiarity of VR in HF is solely due to the high anisotropy of interaction with Ar. Table V presents state resolved cross sections for the $|v=1, j=0\rangle \rightarrow |v=0, j\rangle$ transitions obtained with different number of Legendre polynomials in the angular expansion of PES [Eq. (4)]. The high ($\sim 10-15$) terms in Legendre expansion contribute crucially to transitions from $|v=1, j=0\rangle$ to high rotation levels of $|v=0\rangle$. Quantitative information on the resonance effect may be obtained from Table VI where the state-resolved rate constants obtained for $T=300$ K on two PES' are presented. The rate constants for $|v=1, j=0\rangle \rightarrow |v=0, j=13\rangle$ and $|v=0, j=14\rangle$ transitions constitute the dominant part of the total j-summed rate constant being more than an order of magnitude larger than the transitions to all other j levels.

Table VI shows that the rate constants for VR of HF ($k_{v=1,\, j=0 \rightarrow v=0,\, j}$) calculated on the PAB PES underestimate the values obtained with the DIM PES for low final j values by several orders of magnitude and approach the latter for high j's. This is the consequence of two factors. First, the

TABLE VI. Room temperature rate constants ($cm^3\ s^{-1}$ $molecule^{-1}$) for vibrational relaxation of the $|v=1, j=0\rangle$ level of HF by Ar to various $|v=0, j'\rangle$ states.

j'	$k_{10\rightarrow 0j'}$(DIM PES)	$k_{10\rightarrow 0j'}$(PAB PES)
0	0.546×10^{-19}	0.834×10^{-21}
1	0.105×10^{-18}	0.245×10^{-20}
2	0.103×10^{-18}	0.436×10^{-20}
3	0.153×10^{-18}	0.763×10^{-20}
4	0.212×10^{-18}	0.134×10^{-19}
5	0.354×10^{-18}	0.233×10^{-19}
6	0.572×10^{-18}	0.397×10^{-19}
7	0.957×10^{-18}	0.650×10^{-19}
8	0.156×10^{-17}	0.989×10^{-19}
9	0.249×10^{-17}	0.132×10^{-18}
10	0.338×10^{-17}	0.174×10^{-18}
11	0.424×10^{-17}	0.187×10^{-18}
12	0.703×10^{-17}	0.782×10^{-19}
13	0.330×10^{-16}	0.112×10^{-16}
$\Sigma j'$	0.876×10^{-16}	0.166×10^{-16}

TABLE V. Cross sections ($Å^2$) for $|v=1, j=0\rangle \rightarrow |v=0, j\rangle$ transitions in the Ar+HF collisions obtained with various number of terms (λ) in Legendre expansion (4) of the DIM interaction PES. The collision energy is 300 cm^{-1}.

$j\backslash\lambda$	3	7	10	15	20
0	0.2215×10^{-8}	0.2629×10^{-8}	0.3511×10^{-8}	0.2806×10^{-8}	0.2825×10^{-8}
1	0.5100×10^{-8}	0.6929×10^{-8}	0.6128×10^{-8}	0.6634×10^{-8}	0.6581×10^{-8}
2	0.9882×10^{-9}	0.1908×10^{-8}	0.5184×10^{-8}	0.2470×10^{-8}	0.2517×10^{-8}
3	0.1730×10^{-8}	0.4144×10^{-8}	0.9898×10^{-8}	0.5158×10^{-8}	0.5221×10^{-8}
4	0.1582×10^{-8}	0.3704×10^{-8}	0.6166×10^{-8}	0.3524×10^{-8}	0.3433×10^{-8}
5	0.5553×10^{-9}	0.3663×10^{-8}	0.6368×10^{-8}	0.3806×10^{-8}	0.3636×10^{-8}
6	0.2425×10^{-9}	0.6814×10^{-8}	0.1091×10^{-7}	0.5609×10^{-8}	0.5392×10^{-8}
7	0.9138×10^{-9}	0.9928×10^{-8}	0.1353×10^{-7}	0.4892×10^{-8}	0.4663×10^{-8}
8	0.4351×10^{-9}	0.1838×10^{-7}	0.3410×10^{-7}	0.1035×10^{-7}	0.1027×10^{-7}
9	0.6040×10^{-9}	0.5104×10^{-7}	0.6984×10^{-7}	0.2172×10^{-7}	0.2177×10^{-7}
10	0.1080×10^{-8}	0.1248×10^{-6}	0.1658×10^{-6}	0.4397×10^{-7}	0.4492×10^{-7}
11	0.9058×10^{-9}	0.3573×10^{-6}	0.4421×10^{-6}	0.1162×10^{-6}	0.1195×10^{-6}
12	0.5388×10^{-10}	0.1525×10^{-5}	0.1292×10^{-5}	0.3803×10^{-6}	0.3871×10^{-6}
13	0.1791×10^{-12}	0.4237×10^{-4}	0.5827×10^{-5}	0.2610×10^{-5}	0.2594×10^{-5}
14	0.1567×10^{-17}	0.5013×10^{-6}	0.3444×10^{-5}	0.2372×10^{-5}	0.2354×10^{-5}

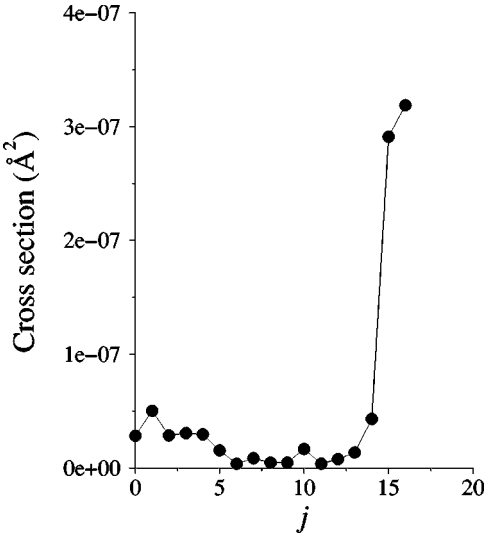

FIG. 7. Cross sections for $|v=1, j=0\rangle \rightarrow |v=0, j\rangle$ transitions in Ar+DF at the collision energy 300 cm^{-1}.

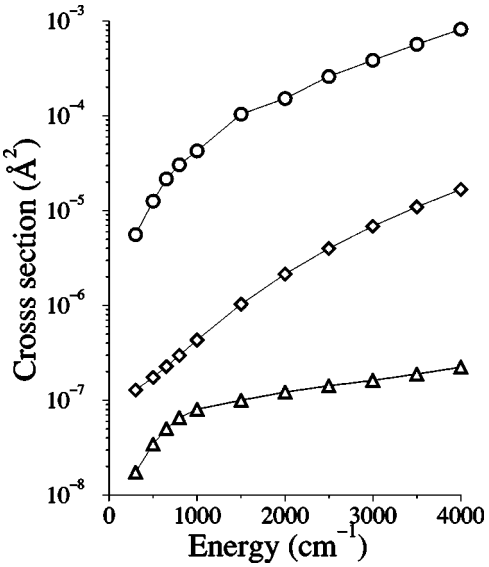

FIG. 8. Cross sections for the $|v=1, j=0\rangle \rightarrow |v=0\rangle$ transitions in Ar+HF from the Coupled States (circles), CC-IOSA (triangles) and effective mass—CC-IOSA (diamonds) calculations.

VR of HF($v=1$) is very slow to low rotational levels of $|v=0\rangle$ and the rate constants should be very sensitive to the interaction potential. Second, the transitions to high rotational levels (~ 13) of $|v=0\rangle$ are determined by high-order terms in Legendre expansion (4) of the interaction potential which have significantly lower magnitude than the first terms. Thus, one should expect a weaker dependence of the $|j=0\rangle \rightarrow |j=13\rangle$ transitions upon the variations of the PES than in the case of $|j=0\rangle \rightarrow |j \sim 0\rangle$ transitions. As a results, since the VR of HF is of a quasiresonant character with transitions to high j levels dominating, even strong variations of the PES do not dramatically change the total VR rates providing the PES remains highly anisotropic.

As follows from Fig. 2(b) there are 16 rotational levels below the first vibrational level in DF and the state $|v=1, j=0\rangle$ is in close resonance with the states $|j=15\rangle$ and $|j=16\rangle$ of $|v=0\rangle$. At the same time the interaction potential of DF with Ar is significantly less anisotropic than in the case of HF+Ar. The calculations (Fig. 7) prove that VR in DF has a similar resonant character to that in HF and the state $|v=1, j=0\rangle$ of DF relaxes mostly to the levels $|j=15\rangle$ and $|j=16\rangle$ of $|v=0\rangle$, although the resonance is less pronounced and there is more structure in the final j dependence of cross sections for VR of DF($v=1, j=0$) than for VR of HF($v=1, j=0$) [cf. Figs. 7 and 6(b)]. Thus, on one hand, the VR rate is suppressed by a decreased anisotropy of the interaction potential but, on the other hand, it is enhanced by the defect of the resonance. Moreover, the initial rotational distribution of DF is broader than that of HF due to a denser spacing of rotational states and one needs to include more cross sections (with the appropriate Boltzmann weighting factors) in order to obtain the converged total VR rates. We tried to evaluate the influence of each of these three factors whose counterplay results in a small isotope HF/DF effect. The lowering of interaction anisotropy decreases the cross sections by a factor 7.0–7.5. The defect of the resonance plays a minor role and increases the VR cross sections by a factor 1.25 at the collision energy 300 cm^{-1}.

The broadening of the initial Boltzmann j distribution increases the relaxation rate by about 3.6 times at $T=300$ K. It is clear that the suppressing effect due to lowering of the interaction anisotropy is the same at all collision energies while the defect of the resonance and the effect of the initial rotational distribution broadening will increase with collision energy and the temperature of the bath gas, correspondingly. So it may be expected that at low temperatures the VR of DF will be smaller than that of HF by at most a factor 2–2.5 and approach (and possibly exceed) the VR of HF at higher temperatures as is observed in the shock tube experiments.[11–13]

Following the works of Banks and Clary[46] and Tanner and Maricq[48] we perform the CC-IOSA calculations of the cross sections for VR in the HF+Ar collisions in order to illustrate the role of molecular rotations in the VR process. Figure 8 depicts the energy dependencies of the cross sections for $|v=1\rangle \rightarrow |v=0\rangle$ transitions in HF obtained with the CC-IOSA method ($\bar{J}=0$) and from the CS calculations for $j=0$. One can see that the IOSA fails dramatically due to the peculiar resonant character of the VR process which can not be reproduced within the IOS approximation for rotational degrees of freedom. Since the CC-IOSA calculations are performed at a number of fixed collision angles Θ the most straightforward way to improve the CC-IOSA results may be to introduce the effective mass for the collision that would account for the internal ro-vibrational energy redistribution in the course of a collision.[24,35] To check this we introduce the effective $\mu^* = \mu/[1+\mu/\mu_{\mathrm{HF}} \sin^2(\Theta)]$ rather than reduced mass in the CC-IOSA. The results of the Effective mass— IOSA calculations shown in Fig. 8 are much closer to the CC-CSA values and their energy dependence is qualitatively the same as of the CC-CSA cross sections. One may hope[35] that by choosing the effective mass in a more appropriate way it is possible to obtain even quantitative agreement with the more accurate CC-CSA data.

In several works the assumption has been made that two-

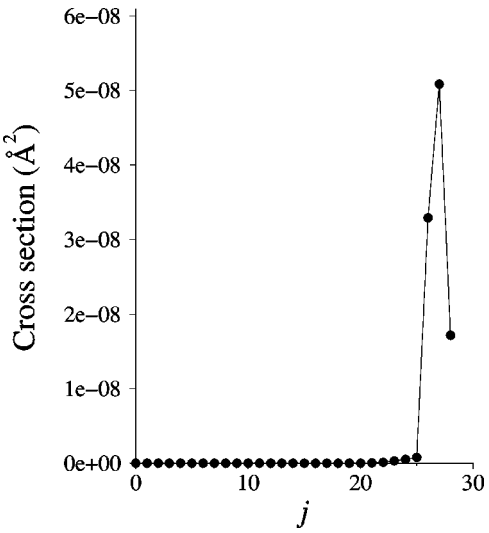

FIG. 9. Cross sections for the $|v=4, j=0\rangle \rightarrow |v=0, j\rangle$ transitions at the collision energy 1300 cm^{-1}.

and multiple quantum vibrational transitions contribute negligibly to the total VR rate. We find, however, that when the difference between two ro-vibrational levels of HF is in close resonance with the collision energy the cross sections for multiple quantum vibrational transitions may be large. Figure 9 illustrates this effect at the collision energy 1300 cm^{-1}. The energy gap between the states $|v=4, j=0\rangle$ and $|v=0, j=27\rangle$ is $\sim$1300 cm^{-1} and it is possible to see the dramatic magnitude of the cross section for this transition in comparison with the transitions to all other levels of the $|v=0\rangle$ manifold. This suggest that although in general the two- and multiple quantum transitions are several orders of magnitude lower than the one-quantum transitions there may be resonance effects that make the former too fast to be neglected.

The results of Fig. 6 and Table VI as well as the quasiresonant character of VR suggest that the low rotational states of $|v=0\rangle$ should be insignificant in the VR process. To investigate this we perform the CC-CS calculations with different number of $|v=0, j\rangle$ states in the basis set (Table VII). The results show that even low-energy rotational channels of $|v=0\rangle$ play a crucial role in VR of $|v=1\rangle$. At the same time the rotational states of $|v=0\rangle$ appear to be insignificant for rotationally inelastic transitions between the states of $|v=1\rangle$ and all states below $|v=1, j=0\rangle$ may be neglected if one is interested in vibrationally elastic ($v=1$) rotational transitions. Thus, the ro-vibrational coupling is important for vibrationally inelastic transitions but plays no role for vibrationally elastic ones.

It is of interest to note that collisional VR and vibrational predissociation of the ArHF complex exhibit many common features. The latter was also found to be of resonant character with a strong propensity for populating the highest accessible rotational level of the HF product.[40] The rate of predissociation, which proceeds through the transfer of one vibrational quantum, scales with v as strongly as v^5 and almost no isotope effect was observed for an ArDF complex for $v=1$.[41] It would be interesting to study such a correspondence in more detail.

IV. SUMMARY

The main results of the present work can be summarized as following:

(1) Accurate close coupling coupled states calculations of the rate constants for rotational relaxation of HF($v=0, j=13$) and vibrational relaxation of HF($v=1$) by Ar are performed for the first time due to availability of a new three-dimensional PES for Ar+HF interaction;
(2) the mechanism of vibrational relaxation of HF($v=1$) is investigated and it is shown that VR is of a quasiresonant character and occurs mostly to two nearest rotational levels of $|v=0\rangle$. This mechanism dominates even at high-collision energies although the resonance peaks are broader and less pronounced than these at small collision energies. The quasiresonant nature of VR is due to large anisotropy of the Ar+HF interaction;
(3) the experimentally observed small HF/DF isotope effect is explained by a counterplay of three factors. Lowering of the interaction anisotropy for DF+Ar decreases the VR rate by about 7–7.5 times while the broadening of the initial rotational distribution of DF in comparison with HF and the defect of the resonance increase the VR rate by a factor 3.5–4 at $T=300$ K. The effect of the initial distribution broadening is expected to increase with temperature and it may lead to a complete disappearance of the isotope effect at higher temperatures;
(4) the cross sections for one quantum relaxation of vibrational levels with $v=1,2,3,4$ are obtained and shown to increase dramatically with v number. The transitions

TABLE VII. Cross sections (Å^2) for vibrationally and rotationally inelastic transitions from the $|v=1, j=0\rangle$ level of HF in collisions with Ar obtained with different number of open channels below the level $|v=0, j=13\rangle$ (N) in the basis set. The maximum number of N is 13.

	Final (v,j)					
N	(0,13)	(0,14)	(0,Σj)	(1,1)	(1,2)	(1,3)
1	0.234×10^{-4}	0.383×10^{-5}	0.273×10^{-4}	10.225	9.834	4.331
3	0.765×10^{-4}	0.583×10^{-5}	0.843×10^{-4}	10.225	9.840	4.331
5	0.580×10^{-4}	0.431×10^{-5}	0.630×10^{-4}	10.225	9.840	4.331
7	0.493×10^{-6}	0.219×10^{-5}	0.281×10^{-5}	10.226	9.840	4.331
9	0.156×10^{-5}	0.212×10^{-5}	0.116×10^{-4}	10.226	9.839	4.335
13	0.259×10^{-5}	0.235×10^{-5}	0.556×10^{-5}	10.197	9.827	4.332

from higher vibrational levels show similar quasiresonant behavior with high rotational levels of $v-1$ mostly populated after a collision. The significant increase of the VR rates with vibrational excitation can be explained by the great increase of the interaction strength with HF bond length elongation;

(5) the multiple quantum vibrational relaxation is found to be negligibly small in general, although the transition cross sections may increase dramatically when the difference between the initial and final states is in close resonance with collision energy;

(6) the crucial role of molecular rotations in the VR process is confirmed by comparison of cross sections from the coupled states calculations and those performed with the infinite-order-sudden approximation for rotational degrees of freedom. It is shown that the CC-IOSA results may be improved by incorporating an effective angle dependent mass that would account for the internal energy redistribution in the diatomic;

(7) the sensitivity of the VR rates to the interaction PES is discussed and it is shown that strong variations of the PES result in relatively small changes of the total VR rate constants which is a consequence of the quasiresonant character of VR with high rotational levels contributing predominantly to the final population distribution;

(8) the role of low energy rotational states of $|v=0\rangle$ in VR is investigated and it is shown that the ro-vibrational coupling is crucial for vibrationally inelastic transitions but it plays no role for vibrationally elastic ones. This suggests that it is possible to perform the close coupling calculations of vibrationally elastic rotational transitions considering only the states of the given v level.

ACKNOWLEDGMENTS

We thank Harald Svedung for providing the modified Buckingham potentials, Stanislav Umanskii for useful discussions, and the Swedish Natural Science Research Council for financial support. A.A.B. also thanks Spanish Ministry of Education and Culture for a sabbatical fellowship.

[1] E. E. Nikitin, S. Ya. Umanskii, and D. V. Shalashilin, Sov. J. Chem. Phys. **9**, 1661 (1992).
[2] N. E. Molevich and A. E. Oraevskii, Khim. Vys. Energ. **21**, 3 (1987).
[3] C. A. Taatjes and S. R. Leone, J. Chem. Phys. **89**, 302 (1988).
[4] E. Arunan, D. Raybone, and D. W. Setser, J. Chem. Phys. **97**, 6348 (1992).
[5] A. Miklavc, N. Marković, G. Nyman, V. Harb, and S. Nordholm, J. Chem. Phys. **97**, 3348 (1992).
[6] S. Clare and A. J. McCaffery, J. Phys. B **33**, 1121 (2000).
[7] J. R. Airey and S. F. Fried, Chem. Phys. Lett. **8**, 23 (1971).
[8] J. K. Hancock and W. H. Green, J. Chem. Phys. **57**, 4515 (1972).
[9] J. J. Hinchen, J. Chem. Phys. **59**, 233 (1973).
[10] S. S. Fried, J. Wilson, and R. L. Taylor, IEEE J. Quantum Electron. **9**, 59 (1973).
[11] J. F. Bott and N. Cohen, J. Chem. Phys. **55**, 3698 (1971).
[12] J. F. Bott and N. Cohen, J. Chem. Phys. **55**, 934 (1973).
[13] J. F. Bott, J. Chem. Phys. **63**, 2253 (1975); **70**, 4123 (1979).
[14] L. S. Blair, W. D. Breshears, and J. L. Schott, J. Chem. Phys. **59**, 1582 (1973).
[15] I. W. M. Smith and D. J. Wrigley, Chem. Phys. Lett. **70**, 481 (1980).
[16] I. W. M. Smith and D. J. Wrigley, Chem. Phys. **63**, 321 (1981).
[17] D. J. Seery, J. Chem. Phys. **58**, 1796 (1973).
[18] R. V. Steele, Jr. and C. B. Moore, J. Chem. Phys. **60**, 2794 (1974).
[19] O. F. J. Losert and B. Schramm, Chem. Phys. Lett. **198**, 355 (1992).
[20] S. R. Leone, J. Phys. Chem. Ref. Data **11**, 953 (1982).
[21] J. J. BelBruno, J. Galfand, and H. Rabitz, J. Chem. Phys. **75**, 4927 (1981).
[22] W. B. Chapman, M. J. Weida, and D. J. Nesbitt, J. Chem. Phys. **106**, 2248 (1997).
[23] C. B. Moore, J. Chem. Phys. **43**, 2979 (1965).
[24] E. E. Nikitin, Teor. Eksp. Khim. **3**, 185 (1967); G. A. Kapralova, E. E. Nikitin, and A. A. Chaikin, Kinet. Katal. **10**, 974 (1969).
[25] G. D. Billing, J. Chem. Phys. **57**, 5241 (1972).
[26] M. Ya. Ovchinnikova and D. V. Shalashilin, Khim. Fiz. **3**, 340 (1984).
[27] M. Y. Ovchinnikova and D. V. Shalashilin, Khim. Fiz. **3**, 643 (1984).
[28] M. Y. Ovchinnikova, Chem. Phys. **93**, 101 (1985).
[29] D. L. Thompson, Chem. Phys. Lett. **84**, 397 (1981).
[30] D. L. Thompson, J. Phys. Chem. **86**, 630 (1982).
[31] F. Battaglia and F. I. Gianturco, Chem. Phys. **55**, 283 (1981).
[32] F. I. Gianturco, U. T. Lamanna, and C. Petrella, Chem. Phys. **78**, 81 (1983).
[33] F. A. Gianturco, E. Semprini, F. Stefani, U. T. Lamanna, and G. Petrella, J. Phys. Chem. **92**, 925 (1988).
[34] R. J. Bienieck, J. Chem. Phys. **79**, 3738 (1983).
[35] T. D. Sewell, S. Nordholm, and A. Miklavc, J. Chem. Phys. **99**, 2567 (1993); N. Marković, T. D. Sewell, S. Nordholm, and A. Miklavc, Chem. Phys. **211**, 277 (1996).
[36] Z. S. Huang, K. W. Jucks, and R. E. Miller, J. Chem. Phys. **85**, 6905 (1986); G. T. Fraser and A. S. Pine, *ibid.* **91**, 633 (1989); S. Davis, J. T. Farrell, D. T. Anderson, and D. J. Nesbitt, Chem. Phys. Lett. **246**, 157 (1995); L. Oudejans, K. Nauta, and R. E. Miller, J. Chem. Phys. **105**, 10410 (1996); C.-C. Chuang, S. N. Tsang, W. Klemperer, and H.-C. Chang, *ibid.* **109**, 8836 (1998).
[37] J. M. Hutson, J. Chem. Phys. **96**, 6752 (1992).
[38] H.-C. Chang, F.-M. Tao, W. Klemperer, C. Healey, and J. M. Hutson, J. Chem. Phys. **99**, 9337 (1993); V. F. Lotrich, H. L. Williams, K. Szalewicz, B. Jeziorski, R. Moszynski, P. E. S. Wormer, and A. van der Avoird, *ibid.* **103**, 6076 (1995); T. van Mourik and T. H. Dunning, Jr., *ibid.* **107**, 2451 (1997); G. Chalasinski, M. M. Szczesniak, and B. Kukawska-Ternawska, *ibid.* **91**, 6677 (1991).
[39] B. L. Grigorenko, A. V. Nemukhin, and V. A. Apkarian, J. Chem. Phys. **104**, 5510 (1996).
[40] A. A. Buchachenko, N. F. Stepanov, B. L. Grigorenko, and A. V. Nemukhin, J. Chem. Phys. **111**, 2470 (1999).
[41] A. A. Buchachenko, N. F. Stepanov, B. L. Grigorenko, and A. V. Nemukhin, Russ. J. Phys. Chem. (to be published).
[42] A. A. Buchachenko, T. Gonzalez-Lezana, M. I. Hernandez, G. Delgado-Barrio, P. Villarreal, and N. F. Stepanov, Chem. Phys. Lett. **269**, 448 (1997); A. A. Buchachenko, N. F. Stepanov, G. Delgado-Barrio, and P. Villarreal, J. Chem. Soc., Faraday Trans. **94**, 2307 (1998).
[43] P. McGuire and D. J. Kouri, J. Chem. Phys. **60**, 2488 (1974); P. McGuire, *ibid.* **62**, 525 (1975); M. H. Alexander and P. McGuire, *ibid.* **64**, 452 (1976).
[44] R. Schinke and G. H. F. Diercksen, J. Chem. Phys. **83**, 4516 (1985).
[45] A. J. Banks, D. C. Clary, and H.-J. Werner, J. Chem. Phys. **84**, 3788 (1986).
[46] A. J. Banks and D. C. Clary, J. Chem. Phys. **86**, 802 (1987).
[47] D. C. Clary, Approximate quantum mechanical calculations on molecular energy transfer and predissociation, in *Supercomputer Algorithms for Reactivity, Dynamics and Kinetics of Small Molecules*, edited by A. Lagana (NATO ASI, Kluwer, 1989), p. 295.
[48] J. J. Tanner and M. M. Maricq, Chem. Phys. **119**, 307 (1988).
[49] R. N. Zare, *Angular Momentum* (Wiley, New York, 1988).
[50] K. Stark and H.-J. Werner, J. Chem. Phys. **104**, 6515 (1996).
[51] H. Svedung, S. Nordholm, and C. Nyeland (in preparation).
[52] J. M. Hutson and S. Green, MOLSCAT computer code 1986, distributed by Collaborative Computational Project No. 6 of the Science and Engineering Research Council, U.K., version 14.
[53] http://www.che.chalmers.se/~roman/ABC3D
[54] D. R. Flower and D. J. Kirkpatrick, J. Phys. B **15**, 1701 (1982).
[55] J. P. Reid, S. J. S. M. Simpson, and H. M. Quiney, J. Chem. Phys. **107**, 9929 (1997); N. Balakrishan, A. Dalgarno, and R. C. Forrey, *ibid.* **113**, 621 (2000).
[56] A. Jörg, A. Degli-Esposti, and H.-J. Werner, J. Chem. Phys. **93**, 8757 (1990).
[57] A. Degli-Esposti and H.-J. Werner, J. Chem. Phys. **93**, 3351 (1990).
[58] J. J. C. Barrett, H. R. Mayne, M. Keil, and L. J. Rawluk, Can. J. Chem. **72**, 985 (1994).